### Title

Coral host cells acidify symbiotic algal microenvironment to promote photosynthesis




### Journal

Proceedings of the National Academy of Sciences of the United States of America, 112(2)

### ISSN

0027-8424



### Authors

Barott, Katie L
Venn, Alexander A
Perez, Sidney O
et al.



### Publication Date

2015-01-13

### DOI

10.1073/pnas.1413483112

Peer reviewed

# Coral host cells acidify symbiotic algal microenvironment to promote photosynthesis

Katie L. Barott[a], Alexander A. Venn[b,c], Sidney O. Perez[a], Sylvie Tambutté[b], and Martin Tresguerres[a,1]

[a]Marine Biology Research Division, Scripps Institution of Oceanography, University of California, San Diego, La Jolla, CA 92093; [b]Marine Biology Department, Centre Scientifique de Monaco, MC-98000 Monaco, Monaco; and [c]Laboratoire Européen Associé 647 "Biosensib," Centre Scientifique de Monaco–Centre National de la Recherche Scientifique, MC-98000 Monaco, Monaco

Edited by George N. Somero, Stanford University, Pacific Grove, CA, and approved November 18, 2014 (received for review July 16, 2014)

**Symbiotic dinoflagellate algae residing inside coral tissues supply the host with the majority of their energy requirements through the translocation of photosynthetically fixed carbon. The algae, in turn, rely on the host for the supply of inorganic carbon. Carbon must be concentrated as $CO_2$ in order for photosynthesis to proceed, and here we show that the coral host plays an active role in this process. The host-derived symbiosome membrane surrounding the algae abundantly expresses vacuolar $H^+$-ATPase (VHA), which acidifies the symbiosome space down to pH ∼4. Inhibition of VHA results in a significant decrease in average $H^+$ activity in the symbiosome of up to 75% and a significant reduction in $O_2$ production rate, a measure of photosynthetic activity. These results suggest that host VHA is part of a previously unidentified carbon concentrating mechanism for algal photosynthesis and provide mechanistic evidence that coral host cells can actively modulate the physiology of their symbionts.**

proton pump | V type $H^+$ ATPase | zooxanthellae | Symbiodinium | carbon concentrating mechanism

Symbiotic corals are the foundation of coral reef ecosystems, providing the complex structural framework that supports the incredible biodiversity of these habitats (1). Coral growth and calcification is supported by the translocation of fixed organic carbon from endosymbiotic dinoflagellate algae of the genus *Symbiodinium*, commonly referred to as zooxanthellae (2). The evolution of this partnership has allowed corals to thrive in oligotrophic tropical marine environments where food and nutrients are generally scarce (2), leading to the rise of coral reefs around 250 million years ago (3). In addition to providing corals with a source of metabolic energy, symbiont photosynthesis is hypothesized to promote coral calcification by supplying precursors for the skeletal organic matrix and by buffering the protons produced during precipitation of the coral's calcium carbonate skeleton (4, 5). Not surprisingly, breakdown of this symbiosis, known as coral bleaching, has serious negative effects on coral physiology and consequently the health of coral reef ecosystems (6, 7). However, despite the clear significance of coral–algae symbiosis in the health of coral reef ecosystems, much remains to be learned about the fundamental cellular mechanisms involved. Understanding these central aspects of coral biology is critical for predicting coral responses to ongoing environmental changes and for developing successful management strategies.

The coral animal consists of two tissue layers: the gastroderm, where the *Symbiodinium* reside, and the ectoderm, which is involved in the exchange of compounds with the external environment and formation of the coral skeleton. *Symbiodinium* are acquired by coral gastrodermal cells via phagocytosis leading to the formation of an intracellular membrane-enclosed compartment known as the "symbiosome" (8). The outer host-derived membrane of the symbiosome goes through a maturation process following alga phagocytosis, whereas the algae develops a membrane complex through which it interacts with the host (2). Due to their intracellular location, *Symbiodinium* rely on the coral host to supply dissolved inorganic carbon (DIC) and nutrients for growth and photosynthesis, all of which must be transported across multiple host membranes to reach the algae. The molecular mechanisms involved in this process remain poorly understood, although identified sources of DIC for photosynthesis include $CO_2$ from host respiration and $HCO_3^-$ from the surrounding seawater (2, 9, 10). Due to the pH-dependent nature of the chemical equilibria between $CO_2$, $HCO_3^-$, and $CO_3^{2-}$, the predominant form of DIC present in the coral cytoplasm (pH > 7) (11) is $HCO_3^-$. This suggests that bicarbonate channels and/or transporters are required to supply *Symbiodinium* with the DIC needed for photosynthesis (12). Furthermore, the low affinity of dinoflagellate Rubisco for $CO_2$ requires that this DIC supply be concentrated via a carbon concentrating mechanism (CCM) in order for photosynthesis to occur (13). *Symbiodinium* have been shown to use carbonic anhydrases (CAs) as part of a CCM during symbiosis (14). The role of the host coral in an algal CCM is as yet unknown, although coral CAs may also be involved. Intriguingly, studies have suggested that the symbiosome compartment is acidic (11, 15). If the pH of the symbiosome lumen was below pH 6.1, the $pK_a$ for the conversion of $CO_2$ and $HCO_3^-$ and the formation of $CO_2$ would be favored. As $CO_2$ can diffuse across the algal plasma membrane, this would promote accumulation of $CO_2$ in the algal cell. However, the pH value of the symbiosome lumen and the mechanisms that generate this proton gradient remain largely unknown.

Due to the potential significance of symbiosome acidification for promoting algal photosynthesis and in regulating the symbiosis,

## Significance

**Coral growth and calcification is supported by sugars acquired from symbiotic algae, allowing corals to thrive in otherwise nutrient-poor environments. This symbiosis depends on the coordinated exchange of compounds between partners, the mechanisms of which are poorly understood. Here we found that coral host cells acidify the microenvironment where the symbiotic algae reside using a proton pump, the V-type $H^+$-ATPase (VHA), which is present in the host membrane surrounding the algae. Acidification of the algal microenvironment by VHA promotes photosynthesis, demonstrating that the coral host can actively regulate symbiont physiology. This work is an important step toward understanding how animal symbioses function and provides mechanistic models that can help understand the capacity of corals to adapt to global climate change.**

Author contributions: K.L.B., A.A.V., S.T., and M.T. designed research; K.L.B. and S.O.P. performed research; K.L.B., A.A.V., S.O.P., S.T., and M.T. analyzed data; and K.L.B. and M.T. wrote the paper.

The authors declare no conflict of interest.

This article is a PNAS Direct Submission.

[1]To whom correspondence should be addressed. Email: mtresguerres@ucsd.edu.

This article contains supporting information online at www.pnas.org/lookup/suppl/doi:10.1073/pnas.1413483112/-/DCSupplemental.

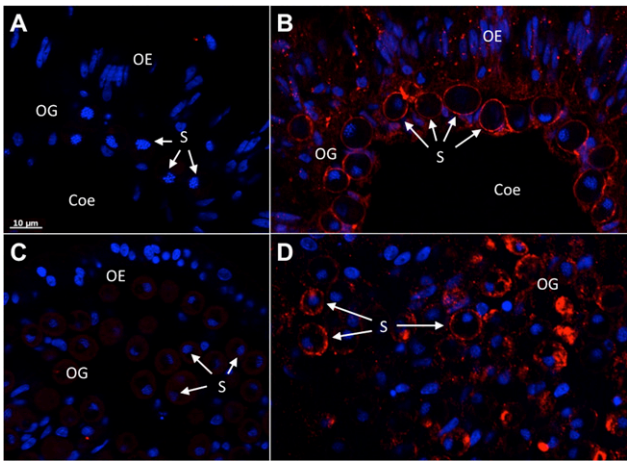


**Fig. 1.** Immunofluorescence localization of VHA in the corals *A. yongei* (*Top*) and *S. pistillata* (*Bottom*). (*A* and *C*) Secondary antibody control. (*B* and *D*) Anti-$VHA_B$ antibody (red). Nuclear staining is shown in blue. Coe, coelenteron; OE, oral ectoderm; OG, oral gastroderm; S, *Symbiodinium*. Arrows indicate examples of *Symbiodinium* cells.

we sought to quantify the pH of the symbiosome lumen and to characterize the cellular mechanisms that regulate its acidification in scleractinian corals. One common mechanism used by cells to acidify intracellular compartments is the V-type proton ATPase (VHA), a membrane transport protein capable of transporting $H^+$ against concentration gradients >100-fold in animals (16) and >1,000-fold in plants (17). Although transcriptomic data indicate that VHA is expressed in corals (18), no information is available on its cellular localization or physiological roles. Here we explored the hypothesis that coral VHA is involved in the acidification of the symbiosome lumen and found that (*i*) VHA is expressed in the host-derived symbiosome membrane of two distantly related coral species representing the two main clades of Scleractinia (Robusta and Complexa); (*ii*) symbiosome pH is highly acidic (pH ∼4), and this acidification is partially dependent on VHA activity; and (*iii*) VHA activity is essential for optimal photosynthetic rate of colonies of both coral species. These results indicate that VHA-dependent symbiosome acidification acts as a CCM that promotes symbiont photosynthesis and implies that the coral host has control over the photosynthetic activity of its algal symbiont. Our findings contribute to a better understanding of the cellular mechanisms of coral–*Symbiodinium* symbiosis, which will facilitate future work on the effects of environmental stress on the physiology of reef-building corals.

## Results and Discussion

**Corals Express VHA in the Host-Derived Symbiosome Membrane.** Representative species of the two major clades of Scleractinia, *Acropora yongei* of the complex clade and *Stylophora pistillata* of the robust clade (19), were chosen for this study. We confirmed that coral VHA was expressed at the transcript level in *A. yongei* by RT-PCR of the VHA B subunit ($VHA_B$; Fig. S1*A*) and in *S. pistillata* by BLAST against an available transcriptome (20) (Fig. S1*E*). Coral VHA was highly conserved with human VHA, including 100% conservation of the anti-$VHA_B$ antibody epitope (Fig. S1*E*). The anti-$VHA_B$ antibody epitope was also highly conserved in *Symbiodinium* sp., with only one amino acid difference (Fig. S1*E*). Expression of the VHA protein was confirmed in both coral species by Western blot with the anti-$VHA_B$ antibody, which recognized a ∼55-kDa protein in *A. yongei* (Fig. S1*B*) and *S. pistillata* (Fig. S1*C*). VHA protein was also detected in cultured *Symbiodinium* (Fig. S1*D*); however, detection required loading of 11-fold more protein, indicating that VHA is expressed at a much lower level in the *Symbiodinium* than in the host coral.

Using immunofluorescence localization in 7-µm sections, we found that VHA was most abundant in the oral gastroderm and was primarily present in the area immediately surrounding the algal cells in both *A. yongei* (Fig. 1 *A* and *B*) and *S. pistillata* (Fig. 1 *C* and *D*). Because the plasma membrane of the coral host cell, its cytoplasm, the symbiosome membrane, and the *Symbiodinium* cell wall and plasma membrane are extremely close together (∼100 nm; Fig. S2), immunolocalization of VHA in isolated cells was required to determine its specific intracellular localization. In isolated coral cells containing one or two algal cells and a host nucleus, VHA staining was consistently observed surrounding the perimeter of the algal cells, but not in the host plasma membrane external to the host nucleus (88/102 cells, or 86%; Fig. 2 *C–F*). In contrast, a minority of free algal cells, as evidenced by the lack of a host nucleus, showed VHA staining (21/186 cells, or 11%; Fig. 2 *G* and *H*), likely in symbiosome membrane remnants. This indicates that VHA is only present surrounding the algal cells when the symbiosis is intact and is therefore most likely found in the host-derived symbiosome membrane. This is the first study, to our knowledge, to directly localize a proton pump in cnidarians, and the presence of VHA in the host-derived symbiosome membrane suggests that it is involved in transporting protons into the symbiosome lumen, and may therefore be involved in regulating physiological processes related to symbiosis. In addition, these results contrast with previous predictions that coral proton pumps are predominantly found in the plasma membrane of various coral cell types (5, 18, 21, 22), with obvious implications about VHA physiological functions.

**The Coral Symbiosome Lumen Is Highly Acidic.** Because VHA is typically involved in acidifying diverse intracellular compartments such as lysosomes, endosomes, synaptic vesicles, and vacuoles, we sought to determine if it similarly acidifies the coral symbiosome compartment. In addition, the pH of the symbiosome lumen in Cnidarians has not been established, and this parameter likely plays an important role in regulating the trafficking of nutrients and signaling molecules between the host coral and its symbiotic algae. To address these questions, we modified a method commonly used to study lysosomal acidification in mammalian systems (23) for use in coral cells involving the dye Lysosensor Green (LSG) DND-189, which accumulates in acidic compartments and fluoresces with increasing intensity as pH decreases ($pK_a$ 5.2).

Freshly isolated *S. pistillata* cells were loaded with 1 µM of LSG and imaged using confocal microscopy. To exclude any damaged symbiosomes from our analysis, only coral gastrodermal cells containing two or more algal cells were used for fluorescence quantification in the symbiosome lumen (Fig. 3 *A–C*). In addition, the use of cells containing multiple symbionts allowed for the visualization of the coral cell cytoplasm while avoiding any overlap of signal from the alga or symbiosome lumen. Following addition of LSG, there was low LSG fluorescence in the cytoplasm of the coral cells (Fig. 3 *A–C*), consistent with previous observations that the cytoplasm of *S. pistillata* gastrodermal cells ranges from pH 7.1–7.4 (11). In contrast, LSG consistently and brightly labeled the symbiosome lumen of isolated *S. pistillata* cells under both light and dark conditions (Fig. 3 *A–C* and Fig. S3), confirming that this compartment is acidic.

Calibration of LSG in live coral cells demonstrated a linear inverse relationship between LSG fluorescence and intracellular pH between pH 4 and 7 (Fig. S4 *A* and *B*); however, LSG fluorescence decreased as pH decreased below pH 4, reaching a minimum at pH 2 (Fig. S4*C*). Because LSG fluorescence in the symbiosome was as high or higher than the brightest point of the calibration curve, we conclude that pH in the symbiosome is ∼4 both in the dark and in the light. However, fluorescence values

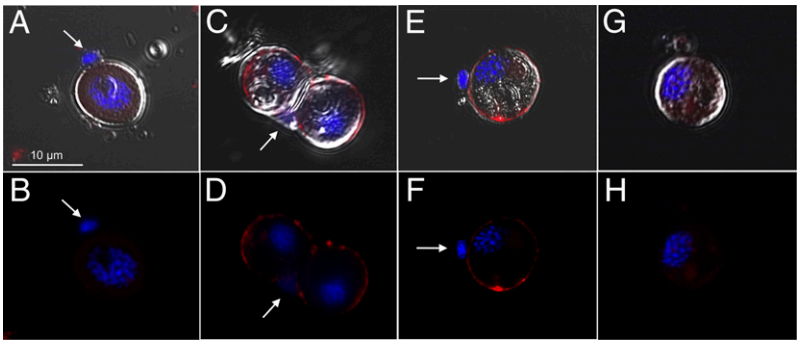


**Fig. 2.** Immunofluorescence localization of VHA in cells isolated from the coral *A. yongei*. (*A* and *B*) Secondary antibody control. (*C* and *D*) Coral cell containing two *Symbiodinium* cells. (*E* and *F*) Coral cell containing a single *Symbiodinium* cell. (*G* and *H*) *Symbiodinium* cell separated from the host. Arrows indicate host nuclei. Anti-$VHA_B$ antibody is shown in red, and nuclear staining is shown in blue. *Top* includes DIC image merged with corresponding fluorescence image in *Bottom* row.

above the brightest point in the calibration prevented determination of the exact pH of the symbiosome. Nonetheless, to our knowledge, this is the most accurate determination of symbiosome lumen pH to date, as previous estimates of symbiosome lumen pH indicated a pH <6 in both anemones and *S. pistillata* but could not determine a more precise value because the pH in this region was out of the range of the dye that was used (11).

**Coral VHA Promotes the Acidic Microenvironment of Symbiosome Lumen.** To determine the role of VHA in acidification of the symbiosome lumen, isolated coral gastrodermal cells loaded with LSG were treated with the highly specific VHA inhibitor bafilomycin (24) and incubated in either light or dark conditions. Addition of 1 μM of bafilomycin induced a significant decrease of LSG fluorescence in the symbiosome lumen (Student's *t* test, $P < 0.05$; Fig. 3*D*). Unfortunately, LSG dye calibration does not allow determining exact pH values, as mentioned above. However, assuming a basal pH of 4 and considering the linear response to pH above that value, inhibition of VHA with bafilomycin is consistent with an increase in average pH of at least 0.40 pH units in the light and 0.60 pH units in the dark (Fig. 3*E*). Because the pH scale is logarithmic, these values correspond to a decrease in $H^+$ activity between 60% and 75%. Furthermore, the pH of the symbiosome was not uniform, instead presenting regions with brighter signal (and therefore more acidic; Fig. S5 *A* and *B*). In these regions, bafilomycin increased pH by 1.2 and 0.8 pH units in the dark and light, respectively (decreases in $H^+$ activity between 95% and 84%, respectively; Fig. S5 *C* and *D*). Interestingly, VHA immunostaining in isolated cells also displayed a punctuated pattern (Fig. 2), suggesting that the regions with the brighter LSG signal are due to increased VHA activity. The pH of the symbiosome lumen did not neutralize in the presence of bafilomycin after 30 min, indicating that either more time was required to reach neutral pH or an additional mechanism(s), such as the symbiosis-dependent *Symbiodinium* P-type $H^+$-ATPase (25), may contribute to acidification of the algal microenvironment.

**Acidification of Algal Microenvironment by Coral VHA Promotes Photosynthesis.** To determine if symbiosome acidification by VHA affects *Symbiodinium* photosynthesis, colonies of *A. yongei* and *S. pistillata* were incubated in the light with bafilomycin and the production of oxygen was measured over time (Fig. 4 *A* and *B*). Inhibition of VHA with bafilomycin led to a significant decrease of net oxygen production in both coral species relative to the DMSO control (*S. pistillata*, 30%; *A. yongei*, 83%; Student's *t* test, $P < 0.05$; Fig. 4 *C* and *D*). In contrast, photosynthesis rates of *Symbiodinium* freshly isolated from *A. yongei* were not significantly affected by bafilomycin (Fig. S6; Student's *t* test, $P > 0.05$), confirming that VHA-stimulated photosynthesis is driven by the host. Altogether, these results demonstrate that the coral host actively promotes *Symbiodinium* photosynthesis through the acidification of the symbiosome lumen by VHA.

We propose that coral VHA is part of a CCM used by corals to promote *Symbiodinium* photosynthesis (26, 27). Coral metabolic energy in the form of ATP present in the coral cytoplasm is consumed by VHA at the symbiosome membrane and used to transport protons from the cytoplasm of the coral cell (pH ~7) to the lumen of the symbiosome (pH~4; Fig. 5*A*). In addition, a plasma membrane $H^+$-ATPase expressed by the algae only during symbiosis (25) may also contribute to the acidification of the symbiosome lumen (Fig. 5*B*). Bicarbonate must also be transported to the symbiosome lumen from the coral cytoplasm, although the mechanisms for this are not known (Fig. 5*C*). Within the symbiosome lumen, the low pH promotes the conversion of $HCO_3^-$ to $CO_2$, which occurs nearly instantaneously in the presence of CAs (Fig. 5) (26, 28). This increases the local concentration of $CO_2$ surrounding the algal cell, which then

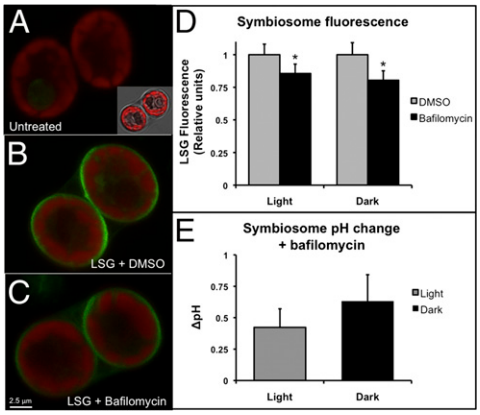


**Fig. 3.** The effect of VHA inhibition by bafilomycin on symbiosome pH in gastrodermal cells isolated from *S. pistillata*. Representative fluorescence images of isolated coral cells containing two symbionts either (*A*) untreated (*Inset* shows light transmission image), (*B*) loaded with 1 μM of LSG and DMSO, or (*C*) in 1 μM of LSG and 1 μM of bafilomycin. Chlorophyll autofluorescence is shown in red. (*D*) LSG fluorescence in the symbiosome following treatment with DMSO or 1 μM of bafilomycin. (*E*) Calculated change in symbiosome pH following treatment with 1 μM of bafilomycin relative to DMSO control. Error bars indicate SEM; $n = 4$ corals, with 30 symbiosomes observed per coral; asterisks denote statistical significance (Student *t* test, $P < 0.05$).

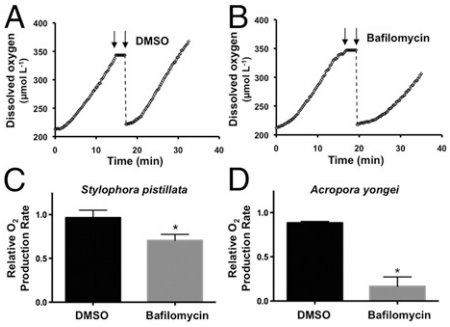


**Fig. 4.** Effect of VHA inhibition on photosynthesis in *S. pistillata* and *A. yongei*. Representative oxygen traces from *S. pistillata* before and after addition of (*A*) DMSO or (*B*) 1 μM of bafilomycin. First arrow indicates pause of data acquisition for treatment addition, and second arrow indicates start of treatment. Relative oxygen production rates following DMSO or bafilomycin treatment for (*C*) *S. pistillata* ($n = 5$) and (*D*) *A. yongei* ($n = 6$). Error bars indicate SEM; asterisks indicate significant differences (Student *t* test, $P < 0.05$).

diffuses across the algal cell wall and plasma membrane. In other organisms, this process may be facilitated by aquaporins; however, it is unknown if *Symbiodinium* express these proteins during symbiosis. Once inside the alga, this carbon must be transported to the site of photosynthesis within the chloroplasts (Fig. 5*D*), which likely requires other CCM(s). Photosynthesis results in the production of oxygen, which diffuses out of the algal cell (Fig. 5*E*), and sugars, which are translocated via unknown mechanisms to the coral host cell (Fig. 5*F*). This VHA-dependent CCM presumably increases the amount of fixed carbon that the host receives, making up for the expenditure of ATP used to drive VHA activity. Furthermore, it may allow the coral host to regulate algal photosynthetic rates by changing VHA activity.

Although symbiosome pH was ∼4 both in light and dark conditions, the exact pH values could not be calculated, and therefore, photosynthesis-induced differences in symbiosome pH cannot be ruled out. It is possible that symbiosme pH is tightly regulated at around 4 pH units despite the alkalinizing effect of photosynthesis on the host cytoplasm (29, 30). This could be achieved, for example, by coordinated modulation of the activity of VHA and other, yet unidentified, acid and base transporters in the symbiosome membrane (Fig. 5).

**Acidification of Symbiosome Lumen May Facilitate Metabolic Exchange Between Host and Symbiont.** Electrochemical gradients across membranes are used in a wide variety of cell and tissue types to drive fundamental physiological processes, including the transport of molecules across membranes such as ions (e.g., $H^+$, $Ca^{2+}$, $Cl^-$, $PO_4^{2-}$, $SO_4^{2-}$), water, and nutrients (e.g., amino acids, glucose), and the formation of action potentials, intercellular signaling, and cell volume regulation (31, 32). In the case of the coral symbiosome, acidification of the symbiosome lumen by VHA results in a sharp proton gradient across the outer symbiosome membrane to the coral cytoplasm and across the algal plasma membrane to the algal cytoplasm of ∼1,000-fold [pH ∼4 (this study) to pH ∼7 (11, 33)] in each direction. These proton gradients likely play an important role in facilitating the import and export of compounds between the symbiosome lumen, the coral cytoplasm, and the algal cytoplasm, making symbiosome acidification a potentially crucial characteristic of host–symbiont communication. For example, low symbiosome pH may drive ammonium transport into the symbiosome lumen by acidic "trapping" as described in the symbiosome of plant–bacterial symbioses (34) and in a variety of animal epithelia (35–37). In the opposite direction, this gradient may help drive the transport of sugars from the symbiosome lumen into the coral cytoplasm. Finally, the continued activity of VHA under dark conditions suggests that symbiosome acidification has additional metabolic roles not directly related to photosynthesis. For example, the maintenance of an acidic microenvironment around the algae may slow down progression of the algal cell cycle due to the pH-sensitive nature of this process. This hypothesis would help explain the physiological mechanisms behind the observed nutrient-independent lengthening of the *Symbiodinium* cell cycle during symbiosis (38).

## Conclusions

Here we found that corals actively promote photosynthesis by their symbiotic algae by acidifying the intracellular microenvironment where the algal cells reside. This is the first time, to our knowledge, that symbiosome pH dynamics in cnidarians has been measured, paving the way for future research on the cellular mechanisms involved in host–symbiont communication and metabolic exchange for this evolutionarily and ecologically important phylum. Determination of symbiosome pH in cnidarians has previously been elusive, partly due to the difficulty of working with live coral cells (11). The pH range of the coral symbiosome lumen estimated here (pH ∼4) is about 100 times lower than previous estimates in cnidarians (pH ∼6) (15) and than in other symbioses (e.g., plant–rhizobium symbiosome compartments range from pH 5.5–6) (39). We show here that this low pH is partially generated by host VHA activity in the symbiosome membrane enveloping the algae. Hosts in other endosymbioses, such as plant–rhyzobium, have also been shown to acidify the symbiosome compartment, although the mechanism differs [plant P-type $H^+$-ATPases (40) vs. coral VHA]. However, the acidic nature of the symbiosome lumen in corals likely shares some similar roles to those of other symbioses, including energizing the transport of various molecules across the symbiosome membrane (41). Detailed physiological mechanisms such as these are important groundwork for understanding and predicting how corals will respond to environmental disturbances such as ocean warming, eutrophication, and acidification.

## Materials and Methods

**Organisms.** Colonies of the corals *A. yongei* and *S. pistillata* were maintained in flow-through seawater at 26 °C and 25 °C, respectively, with a 12:12 h

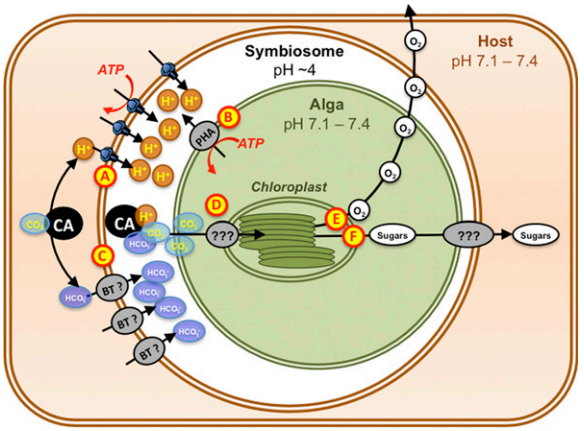


**Fig. 5.** Model of host-driven CCM in scleractinian corals. $H^+$ is transported into the symbiosome by coral VHA (blue icon) (*A*) and algal P-type $H^+$-ATPase (PHA) (25) (*B*), whereas $HCO_3^-$ enters via unidentified $HCO_3^-$ transporter(s) (BT?) (*C*). In the symbiosome, CA catalyzes the dehydration of $H^+$ and $HCO_3^-$ into $CO_2$ (14), which diffuses into the algal cell. Once $CO_2$ enters the alga, it is transported by unknown mechanisms (*D*) to the site of carbon fixation. The resulting $O_2$ diffuses out of the cell (*E*), whereas sugars are translocated to the host via unknown mechanisms (*F*).

light:dark cycle. *S. pistillata* colonies contained *Symbiodinium* sp. clade A; *A. yongei* colonies contained predominantly *Symbiodinium* sp. clade C. *Symbiodinium* sp. clade F were cultured in F/4 media and kept at 26 °C with a 12:12 h light:dark cycle. All organisms were sampled during the light for analysis of protein expression and localization.

**Confirmation of Coral VHA Gene Expression.** Coral tissue was removed from the skeleton and homogenized using an airbrush (80 psi) with a "homogenization buffer" made of S22 Buffer (450 mM NaCl, 10 mM KCl, 58 mM $MgCl_2$, 10 mM $CaCl_2$, 100 mM Hepes, pH 7.8) (42) supplemented with a protease inhibitor mixture (Sigma) and phosphotase inhibitor (PhosStop; Roche Applied Science). The resulting tissue slurry was passed through a 21-G syringe to shear the mucus and placed in TRIzol. Total RNA was extracted according to the manufacturer's directions. Total RNA was converted to cDNA using the SuperScript III First Strand Synthesis System for RT-PCR (Invitrogen) using oligo-dT or random hexamer primers according to the manufacturer's directions. The resulting cDNA was used as the template for RT-PCR for the $VHA_B$ gene. Coral-specific primers (101F, 5′-TTCTGGTGTGAATGGGCCTC-3′, and 1055R, 5′-TCTGGGATGGGATGGGTGAT-3′) were designed against the putative $VHA_B$ gene from the *Acropora digitifera* genome (43). The sequence was amplified by the following protocol: 94 °C 2 min, 10 cycles of 94 °C for 30 s, 58–0.5 °C per cycle for 30 s, 72 °C for 60 s, then 30 cycles of 94 °C for 30 s, 53 °C for 30 s, 72 °C for 60 s, followed by a final extension at 72 °C for 5 min. Resulting PCR products were purified using the DNA Clean & Concentrator kit (Zymo Research) and sequenced by Retrogen.

**Antibodies.** Custom rabbit polyclonal anti-$VHA_B$ antibodies were developed using a peptide antigen matching a conserved region of the $VHA_B$ subunit (AREEVPGRRGFPGY; Genscript USA, Inc.). These antibodies specifically recognize $VHA_B$ by Western blot and immunofluorescence in a variety of species including sharks (44, 45) and marine worms (46). Based on conservation of the antigen epitope in *Acropora* spp. and *S. pistillata* (Fig. S1) and peptide preabsorption controls (Figs. S1 and S7), these antibodies also specifically recognize $VHA_B$ protein in corals.

**Confirmation of VHA Protein Expression.** Coral tissue was homogenized as described above. *Symbiodinium* cells were pelleted from the culture media by centrifugation at 3,000 × *g* for 10 min at room temperature, resuspended in a small volume of homogenization buffer, and lysed by sonication. Protein concentrations for all samples were determined using the Bradford Assay with a BSA standard curve. Tissue homogenates were then incubated in Laemmli Sample buffer with 5% (vol/vol) β-mercaptoethanol for 15 min at 70 °C and loaded on an SDS/PAGE gel. Following gel separation, proteins were transferred to a PVDF membrane using a TurboBlot (BioRad). The membrane was blocked for 1 h on an orbital shaker in Tris-buffered saline with 0.1% Triton-X (TBS-T) and 5% fat-free milk at room temperature, and subsequently incubated overnight at 4 °C with $VHA_B$ antibodies (1.5 $\mu g \cdot ml^{-1}$). The membrane was then washed three times in TBS-T for 10 min each, then stained with the secondary antibodies (1:10,000; goat anti-rabbit HRP; BioRad) for 1 h at room temperature with shaking. The membrane was washed again, and bands were visualized using the ECL Prime Western Blot Detection Reagent (Amersham), then imaged with a BioRad Chemidoc Imaging system.

**Immunolocalization of VHA.** Coral tissue was prepared as described previously (42). Briefly, samples were fixed overnight in S22 buffer with 3% paraformaldehyde at 4 °C. Corals were then decalcified in Ca-free S22 buffer with 0.5 M EDTA, and the buffer was replaced daily until the skeleton was completely dissolved (~7–10 d). Tissue was then dehydrated, embedded in paraffin, and sectioned (6 μM). Isolated coral cells were prepared from *A. yongei* colonies as described previously (11). Cells then were fixed in S22 buffer with 4% paraformaldehyde for 15 min on ice. Cells were pelleted to remove the fixative and resuspended in S22 buffer, then spread onto glass slides and air-dried. In some cases, several layers of cells were added to each slide to increase the cell concentration. Tissue sections were rehydrated, and both sections and isolated cells were permeabilized in 0.2% triton-x in PBS for 60 or 10 min, respectively. Samples were then blocked for 1 h with 2% normal goat serum in PBS, stained with the anti-$VHA_B$ antibody (3 $\mu g \cdot ml^{-1}$) overnight at 4 °C, incubated with the secondary antibody (goat anti-rabbit Alexa555), and stained with Hoescht to visualize DNA. Controls were treated as above except no primary antibody was used. Immunofluorescence was detected using an epifluorescence microscope (Zeiss AxioObserver Z1) connected to a metal halide lamp and appropriate filters. Some images were captured using structured illumination (Zeiss Apotome2). Digital images were adjusted, for brightness and contrast only, using Zeiss Axiovision software and Adobe Photoshop.

Quantification of VHA staining in isolated cells was conducted on randomly selected cells from three separate preparations (288 cells total). First, *Symbiodinium* cells were identified based on their shape and chlorophyll autofluorescence in the green channel. Next, the number of nuclei was counted based on Hoescht staining. Finally, the presence/absence and localization of VHA immunostaining was determined based on the red fluorescence from the secondary antibodies. Cells were divided into three subtypes: isolated *Symbiodinium* (one observable algal nucleus), a single *Symbiodinium* within a coral host cell (one algal nucleus and one host nucleus), or two *Symbiodinium* within a coral host cell (two algal nuclei and one host nucleus) (Fig. 2).

**TEM Histology.** *A. yongei* fragments were fixed overnight at 4 °C in 2% paraformaldehyde and 2.5% glutaraldehyde in S22 buffer (42). Corals were then decalcified in Ca-free S22 with 0.5% paraformaldehyde at 4 °C. Decalcification buffer was replaced daily for ~1–2 wk until the skeleton had completely dissolved. Fixed and decalcified coral tissue samples were immersed in modified Karnovsky's fixative (2.5% glutaraldehyde and 2% paraformaldehyde in 0.15 M sodium cacodylate buffer, pH 7.4) for at least 4 h, postfixed in 1% osmium tetroxide in 0.15 M cacodylate buffer for 1 h, and stained en bloc in 2% uranyl acetate for 1 h. Samples were dehydrated in ethanol, embedded in Durcupan epoxy resin (Sigma-Aldrich), sectioned at 50–60 nm on a Leica UCT ultramicrotome, and picked up on Formvar and carbon-coated copper grids. Sections were stained with 2% uranyl acetate for 5 min and Sato's lead stain for 1 min. Grids were viewed using a JEOL 1200EX II (JEOL) transmission electron microscope and photographed using a Gatan digital camera (Gatan).

**Symbiosome pH Quantification.** To determine symbiosome pH, gastrodermal cells were isolated from *S. pistillata* as described previously (11) and loaded with 1 μM of LSG D-189 (Life Technologies) dissolved in 0.45 μM of filtered seawater (FSW) for 30 min in the dark. Cells were pelleted by centrifugation to remove the dye and resuspended in FSW supplemented with either 1 μM of bafilomycin A1 or an equivalent volume of DMSO. Cells were then incubated for 10 min in the dark or 20 min in the light (290 μM) and imaged using a confocal microscope (Leica SP5). An excitation wavelength of 405 nm was used to minimize excitation of endogenous GFP, and emission was recorded at 505 nm. Only intact coral cells containing two or more algal symbionts were imaged to ensure that only intact symbiosomes were included in the analysis. These cells were selected under bright field to avoid observer bias based on LSG fluorescence. The microscope was focused at the cell "equator," where the diameter of the *Symbiodinium* was the largest. Each cell was then imaged once with the laser to avoid bleaching of LSG fluorescence. The microscope was then returned to bright field mode, a separate field of view was selected, and the process was repeated for at least 15 cells. A total of four cell preparations taken from four different colonies were used for both light and dark experiments, resulting in the analysis of 60 coral gastrodermal cells and at least 120 symbiosomes for each treatment. The average LSG fluorescence intensity was determined from the images by drawing a region of interest around the entire symbiosome lumen, excluding the algal cell. The average symbiosome fluorescence for each coral cell was determined by averaging the symbiosome fluorescence of the symbionts contained within that coral cell. For LSG calibration, a range of pH buffers (pH 2–7) was used in conjunction with the ionophore nigericin (30 μM) to equilibrate intracellular pH in isolated coral cells as previously described, with the exception that Mes buffer was used for calibration buffers of pH 2–5.5 instead of Pipes (11). These cells were loaded with 1 μM of LSG for in vivo calibration, and the intracellular LSG fluorescence was examined under either light or dark conditions as described above. This LSG calibration method has previously been used in mammalian lysosome pH studies (23). The same laser intensity, gain, and magnification settings were used for all dark experiments and calibrations. The laser intensity and gain were adjusted for the light calibration to avoid overexposure under the "dark settings," and these new "light settings" were held constant for each step of the light calibration. Settings were also kept consistent within each light experiment (i.e., each DMSO and corresponding bafilomycin treatment), but gain had to be adjusted between some cell preparations to avoid overexposure. The magnitude of the pH change observed following bafilomycin treatment was calculated from the slope of the corresponding standard curve: For the observed delta fluorescence, the corresponding delta pH was calculated.

**Oxygen Production Measurements.** *A. yongei* nubbins 1.5–2 cm in length were collected from different colonies of a clonal population ($n = 6$) at Scripps Institution of Oceanography, University of California, San Diego. Corals were allowed to heal for 5 d before the experiment. Freshly isolated *Symbiodinium* (FIS) were prepared by homogenizing *A. yongei* tissue in FSW with an air-brush (80 psi). The homogenate was then passed although a 21-G needle with a syringe three times to shear the mucus and then passed through a 100-μM cell strainer. *Symbiodinium* were pelleted by centrifugation at 750 × *g* for 1 min and resuspended in FSW, and this process was repeated three times to remove coral cells and debris. The cells were then filtered through a 40-M cell strainer, pelleted at 750 × *g* for 2 min, and resuspended in FSW. Net oxygen production for *A. yongei* and FIS was measured in sealed glass chambers at 26 °C and 150 μmol photons $m^{-2}{\cdot}s^{-1}$ irradiance using a Clark-type oxygen electrode (Unisense) that was calibrated with an anoxic solution (0.1 M NaOH, 0.1 M sodium ascorbate) and 100% air-saturated seawater. Experimental chambers were stirred with an internal magnetic stir bar, and data were recorded using the accompanying MicOx software. Corals or FIS were treated with either DMSO as a carrier control or 500 nM bafilomycin, which was added to the sample by injection with a gas-tight syringe through a capillary port in the lid of the chamber. *S. pistillata* nubbins 1.5–2 cm in length were collected from the same colony at the Centre Scientifique de Monaco and allowed to heal for 2 wk before the experiment. Net oxygen production for *S. pistillata* was measured in sealed glass chambers using an oxygen optode system (OXY-4, Presens) calibrated with an anoxic solution of 1% sodium sulfite and 100% air-saturated seawater. The experiment was conducted at 25 °C and 170 μmol photons $m^{-2}{\cdot}s^{-1}$ irradiance. Oxygen production was measured for 15 min in untreated seawater, followed by a complete replacement with either DMSO or 1 μM of bafilomycin in seawater. Oxygen production was recorded for another 15 min following treatment addition. Oxygen production rates were determined by taking the slope of the linear portion of the curves before and after treatment addition (Fig. 4 *A* and *B*). Relative oxygen production rates were determined by dividing the treated (DMSO or bafilomycin) oxygen production rate by the untreated oxygen production rate of the same nubbin or FIS sample.

**ACKNOWLEDGMENTS.** We thank Dimitri Deheyn and Jenny Tu for providing access to *A. yongei* colonies and Michael Latz for providing *Symbiodinium* cultures. This work was supported by National Science Foundation Grants EF-1220641 (to M.T.) and OCE-1226396 (to K.L.B.), Alfred P. Sloan Research Fellowship Grant BR2013-103 (to M.T.), and the Government of the Principality of Monaco.

1. Knowlton N, et al. (2010) *Life in the World's Oceans: Diversity, Distribution, and Abundance* (John Wiley and Sons West Sussex, UK), pp 65–77.
2. Davy SK, Allemand D, Weis VM (2012) Cell biology of cnidarian-dinoflagellate symbiosis. *Microbiol Mol Biol Rev* 76(2):229–261.
3. Muscatine L, et al. (2005) Stable isotopes (δ13C and δ15N) of organic matrix from coral skeleton. *Proc Natl Acad Sci USA* 102(5):1525–1530.
4. Moya A, et al. (2006) Study of calcification during a daily cycle of the coral Stylophora pistillata: Implications for 'light-enhanced calcification'. *J Exp Biol* 209(Pt 17): 3413–3419.
5. Allemand D, et al. (2004) Biomineralisation in reef-building corals: From molecular mechanisms to environmental control. *C R Palevol* 3(6-7):453–467.
6. Weis VM (2008) Cellular mechanisms of Cnidarian bleaching: Stress causes the collapse of symbiosis. *J Exp Biol* 211(Pt 19):3059–3066.
7. Baker AC, Glynn PW, Riegl B (2008) Climate change and coral reef bleaching: An ecological assessment of long-term impacts, recovery trends and future outlook. *Estuar Coast Shelf Sci* 80(4):435–471.
8. Roth E, Jeon K, Stacey G (1988) *Molecular Genetics of Plant-Microbe Interactions* (American Phytopathological Society Press, St. Paul, MN), pp 220–225.
9. Goiran C, Al-Moghrabi S, Allemand D, Jaubert J (1996) Inorganic carbon uptake for photosynthesis by the symbiotic coral/dinoflagellate association I. Photosynthetic performances of symbionts and dependence on sea water bicarbonate. *J Exp Mar Biol Ecol* 199(2):207–225.
10. Al-Moghrabi S, Goiran C, Allemand D, Speziale N, Jaubert J (1996) Inorganic carbon uptake for photosynthesis by the symbiotic coral-dinoflagellate association II. Mechanisms for bicarbonate uptake. *J Exp Mar Biol Ecol* 199(2):227–248.
11. Venn AA, et al. (2009) Imaging intracellular pH in a reef coral and symbiotic anemone. *Proc Natl Acad Sci USA* 106(39):16574–16579.
12. Allemand D, Furla P, Bénazet-Tambutté S (1998) Mechanisms of carbon acquisition for endosymbiont photosynthesis in Anthozoa. *Can J Bot* 76(6):925–941.
13. Leggat W, et al. (2002) Dinoflagellate symbioses: Strategies and adaptations for the acquisition and fixation of inorganic carbon. *Funct Plant Biol* 29(3):309–322.
14. Bertucci A, et al. (2013) Carbonic anhydrases in anthozoan corals—A review. *Bioorg Med Chem* 21(6):1437–1450.
15. Rands M, Loughman B, Douglas A (1993) The symbiotic interface in an alga-invertebrate symbiosis. *Proc Biol Sci* 253(1337):161–165.
16. Stevens TH, Forgac M (1997) Structure, function and regulation of the vacuolar (H+)-ATPase. *Annu Rev Cell Dev Biol* 13(1):779–808.
17. Müller M, Irkens-Kiesecker U, Rubinstein B, Taiz L (1996) On the mechanism of hyperacidification in lemon. Comparison of the vacuolar H(+)-ATPase activities of fruits and epicotyls. *J Biol Chem* 271(4):1916–1924.
18. Kaniewska P, et al. (2012) Major cellular and physiological impacts of ocean acidification on a reef building coral. *PLoS ONE* 7(4):e34659.
19. Budd AF, Romano SL, Smith ND, Barbeitos MS (2010) Rethinking the phylogeny of scleractinian corals: A review of morphological and molecular data. *Integr Comp Biol* 50(3):411–427.
20. Karako-Lampert S, et al. (2014) Transcriptome analysis of the scleractinian coral Stylophora pistillata. *PLoS ONE* 9(2):e88615.
21. Moya A, et al. (2012) Whole transcriptome analysis of the coral Acropora millepora reveals complex responses to $CO_2$-driven acidification during the initiation of calcification. *Mol Ecol* 21(10):2440–2454.
22. Jokiel PL (2011) The reef coral two compartment proton flux model: A new approach relating tissue-level physiological processes to gross corallum morphology. *J Exp Mar Biol Ecol* 409(1-2):1–12.
23. Zhang Y, Li X, Grassmé H, Döring G, Gulbins E (2010) Alterations in ceramide concentration and pH determine the release of reactive oxygen species by Cftr-deficient macrophages on infection. *J Immunol* 184(9):5104–5111.
24. Bowman EJ, Siebers A, Altendorf K (1988) Bafilomycins: A class of inhibitors of membrane ATPases from microorganisms, animal cells, and plant cells. *Proc Natl Acad Sci USA* 85(21):7972–7976.
25. Bertucci A, Tambutté E, Tambutté S, Allemand D, Zoccola D (2010) Symbiosis-dependent gene expression in coral-dinoflagellate association: Cloning and characterization of a P-type H+-ATPase gene. *Proc Biol Sci* 277(1678):87–95.
26. Weis VM (1993) Effect of dissolved inorganic carbon concentration on the photosynthesis of the symbiotic sea anemone Aiptasia pulchella Carlgren: Role of carbonic anhydrase. *J Exp Mar Biol Ecol* 174(2):209–225.
27. Leggat W, Badger MR, Yellowlees D (1999) Evidence for an inorganic carbon-concentrating mechanism in the symbiotic dinoflagellate Symbiodinium sp. *Plant Physiol* 121(4):1247–1256.
28. Weis VM, Smith GJ, Muscatine L (1989) A "CO2 supply" mechanism in zooxanthellate cnidarians: Role of carbonic anhydrase. *Mar Biol* 100(2):195–202.
29. Laurent J, Tambutté S, Tambutté É, Allemand D, Venn A (2012) The influence of photosynthesis on host intracellular pH in scleractinian corals. *J Exp Biol*. Available at http://jeb.biologists.org/content/early/2012/12/18/jeb.082081. Accessed January 16, 2013.
30. Gibbin EM, Putnam HM, Davy SK, Gates RD (2014) Intracellular pH and its response to CO2-driven seawater acidification in symbiotic versus non-symbiotic coral cells. *J Exp Biol* 217(Pt 11):1963–1969.
31. Palmgren MG, Nissen P (2011) P-type ATPases. *Annu Rev Biophys* 40(1):243–266.
32. Blanco G, Mercer RW (1998) Isozymes of the Na-K-ATPase: Heterogeneity in structure, diversity in function. *Am J Physiol* 275(5 Pt 2):F633–F650.
33. Gibbin EM, Davy SK (2013) Intracellular pH of symbiotic dinoflagellates. *Coral Reefs* 32(3):859–863.
34. Day DA, Poole PS, Tyerman SD, Rosendahl L (2001) Ammonia and amino acid transport across symbiotic membranes in nitrogen-fixing legume nodules. *Cell Mol Life Sci* 58(1):61–71.
35. Weihrauch D, Morris S, Towle DW (2004) Ammonia excretion in aquatic and terrestrial crabs. *J Exp Biol* 207(Pt 26):4491–4504.
36. Wright PA, Wood CM (2009) A new paradigm for ammonia excretion in aquatic animals: Role of Rhesus (Rh) glycoproteins. *J Exp Biol* 212(Pt 15):2303–2312.
37. Weiner ID, Verlander JW (2011) Role of NH3 and NH4+ transporters in renal acid-base transport. *Am J Physiol Renal Physiol* 300(1):F11–F23.
38. Smith GJ, Muscatine L (1999) Cell cycle of symbiotic dinoflagellates: Variation in G1 phase-duration with anemone nutritional status and macronutrient supply in the Aiptasia pulchella–Symbiodinium pulchrorum symbiosis. *Mar Biol* 134(3):405–418.
39. Perez-Galdona R, Kahn ML (1994) Effects of organic acids and low pH on Rhizobium meliloti 104A14. *Microbiology* 140(Pt 5):1231–1235.
40. Fedorova E, et al. (1999) Localization of H(+)-ATPases in soybean root nodules. *Planta* 209(1):25–32.
41. Udvardi M, Poole PS (2013) Transport and metabolism in legume-rhizobia symbioses. *Annu Rev Plant Biol* 64(1):781–805.
42. Puverel S, et al. (2005) Antibodies against the organic matrix in scleractinians: A new tool to study coral biomineralization. *Coral Reefs* 24(1):149–156.
43. Shinzato C, et al. (2011) Using the Acropora digitifera genome to understand coral responses to environmental change. *Nature* 476(7360):320–323.
44. Roa JN, Munévar CL, Tresguerres M (2014) Feeding induces translocation of vacuolar proton ATPase and pendrin to the membrane of leopard shark (Triakis semifasciata) mitochondrion-rich gill cells. *Comp Biochem Physiol A Mol Integr Physiol* 174:29–37.
45. Tresguerres M, et al. (2010) Bicarbonate-sensing soluble adenylyl cyclase is an essential sensor for acid/base homeostasis. *Proc Natl Acad Sci USA* 107(1):442–447.
46. Tresguerres M, Katz S, Rouse GW (2013) How to get into bones: Proton pump and carbonic anhydrase in Osedax boneworms. *Proc Biol Sci* 280(1761):20130625.

# Supporting Information

## Barott et al. 10.1073/pnas.1413483112

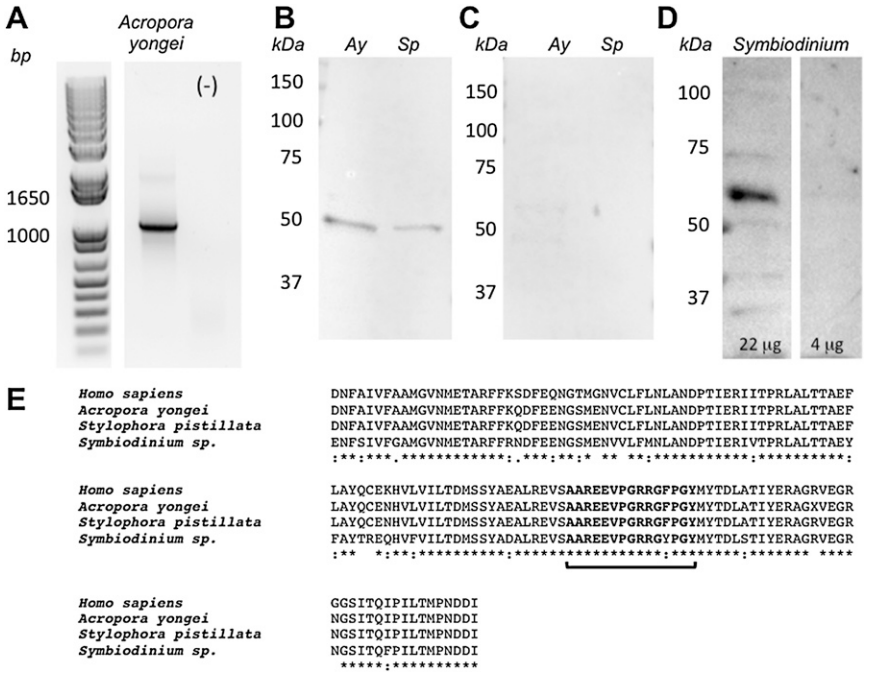


**Fig. S1.** Expression and conservation of VHA in corals. (*A*) RT-PCR amplification of VHA from *A. yongei* cDNA. Western blot detection of VHA in (*B*) *A. yongei* (Ay) and *S. pistillata* (Sp) using anti-$VHA_B$ antibodies, (*C*) *A. yongei* and *S. pistillata* using anti-$VHA_B$ antibodies preabsorbed with 200-fold excess antigen peptide overnight before performing the Western blot with 2 µg of total protein in each lane, and (*D*) cultured *Symbiodinium* using anti-$VHA_B$ antibodies. The two panels shown (22 µg protein vs. 4 µg protein) are different lanes from the same gel. (*E*) Alignment of the human VHA protein sequence (*Homo sapiens*; P15313.3) with the predicted protein sequences derived from the *A. yongei* cDNA sequence in *A*, the *S. pistillata* transcriptome (1), and the dinoflagellate *Symbiodinium* sp. A2 (TSA; GBGW01000407.1). The epitope region of the mammalian anti-$VHA_B$ antibody is indicated by the bracket, with conserved amino acids highlighted in bold.

1. Karako-Lampert S, et al. (2014) Transcriptome analysis of the scleractinian coral *Stylophora pistillata*. *PLoS ONE* 9(2):e88615.

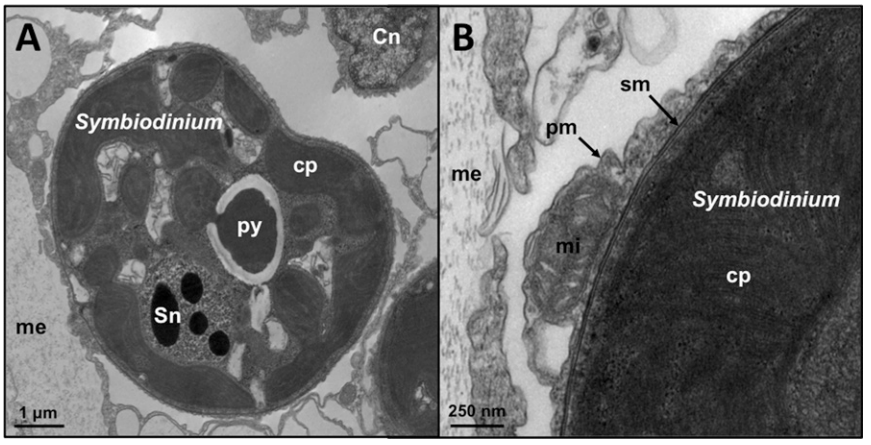


**Fig. S2.** Transmission electron micrographs of the *A. yongei* gastroderm. (*A*) *Symbiodinium* cell within the oral gastroderm. (*B*) Detail of the host plasma and symbiosome membranes surrounding a *Symbiodinium* cell. Cn, coral nucleus; cp, chloroplast; me, mesoglea; mi, mitochondrion; pm, plasma membrane; py, pyrenoid; sm, symbiosome membrane; Sn, *Symbiodinium* nucleus.

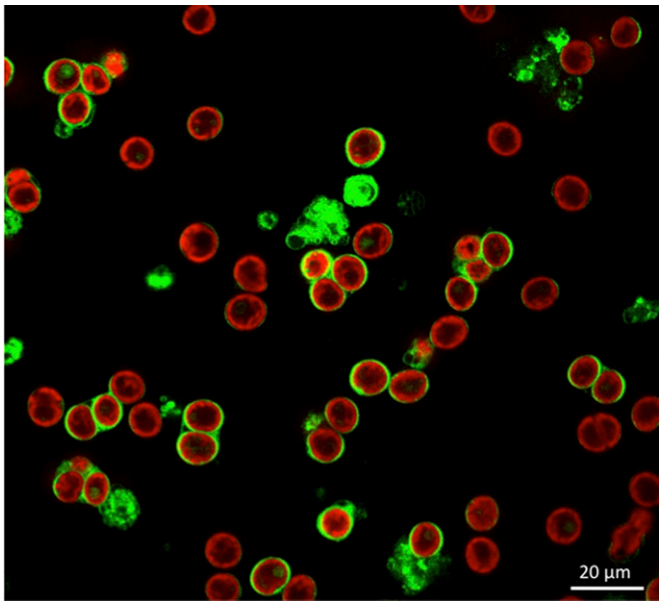


**Fig. S3.** Isolated *S. pistillata* cells loaded with 1 µM of LSG (green). Isolated cells include free *Symbiodinium* cells dissociated from the host symbiosome that lack LSG staining, as well as intracellular *Symbiodinium* cells showing strong LSG staining in the symbiosome. Red indicates chlorophyll autofluorescence.

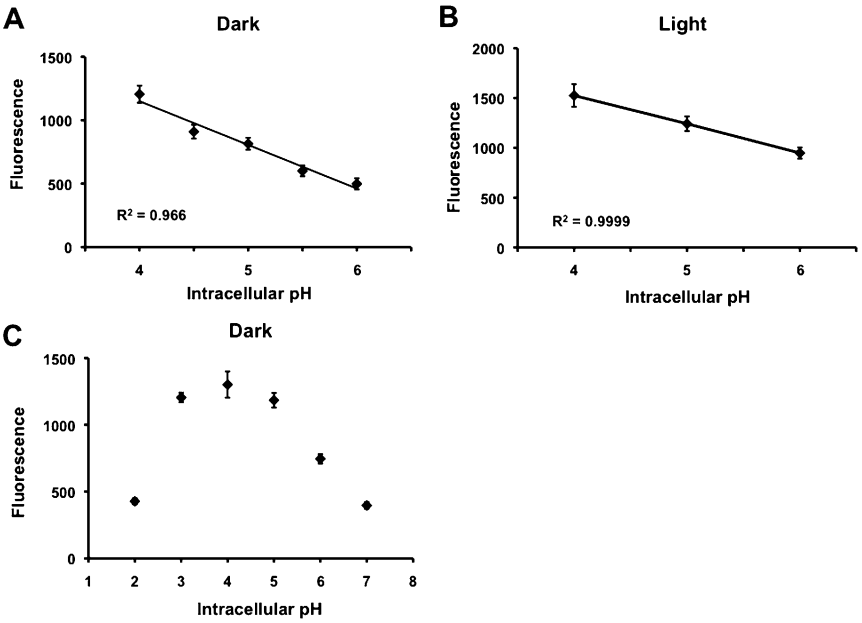


**Fig. S4.** Calibration of gastrodermal cells loaded with 1 µM of LSG and the indicated intracellular pH. (*A*) Linear calibration range in the dark. (*B*) Linear calibration range in the light. (*C*) Extended calibration at low pH in the dark. $n = 15$; error bars indicate SEM. Note that fluorescence values are not directly comparable between calibrations due to image acquisition under different microscope settings.

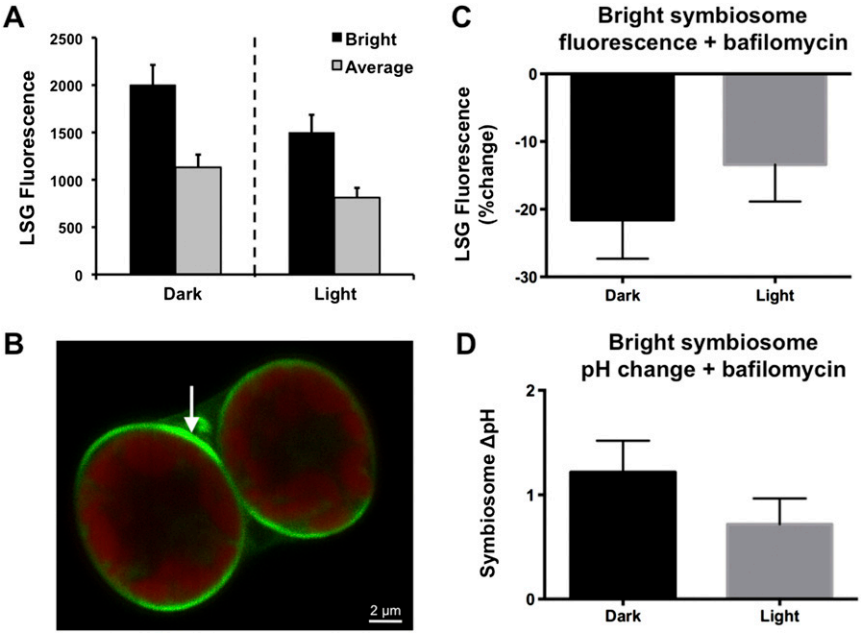


**Fig. S5.** The effect of VHA inhibition by bafilomycin on pH in bright symbiosome regions of gastrodermal cells isolated from *S. pistillata*. (*A*) Comparison of average LSG fluorescence across the entire symbiosome versus bright regions. Dashed line indicates that fluorescence values between light and dark conditions are not directly comparable due to image acquisition under different microscope settings. (*B*) Example of bright region within one symbiosome, indicated by arrow. (*C*) Change in LSG fluorescence in the bright symbiosome regions following treatment with 1 µM of bafilomycin relative to DMSO control. (*D*) Calculated change in bright symbiosome region pH following treatment with 1 µM of bafilomycin relative to DMSO control; calculation was based on the LSG standard curve for either the light or dark, respectively. Error bars indicate SEM.

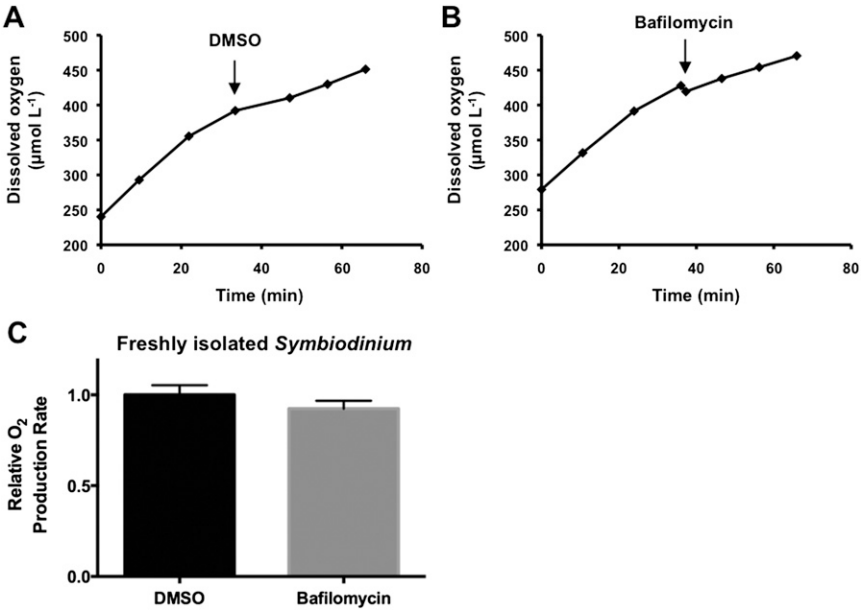


**Fig. S6.** Effect of VHA inhibition on photosynthesis rates of FIS cells from the coral *A. yongei*. Representative oxygen traces from FIS before and after addition of (*A*) DMSO or (*B*) 500 nM of bafilomycin. (*C*) Oxygen production rates relative to the DMSO control. Arrows indicate timing of treatment addition. Error bars indicate SEM; $n = 5$; Student $t$ test, $P > 0.05$.

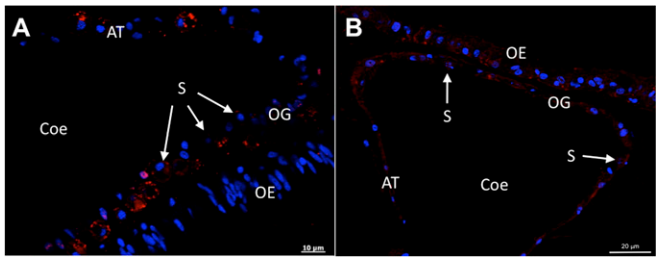


**Fig. S7.** Antigen peptide preabsorption controls for anti-$VHA_B$ antibodies in (*A*) *A. yongei* and (*B*) *S. pistillata*. Anti-$VHA_B$ antibodies (red) were preabsorbed with 100-fold excess antigen peptide overnight before immunostaining was performed. Nuclear staining is shown in blue. AT, aboral tissue; Coe, coelenteron; OE, oral ectoderm; OG, oral gastroderm; S, *Symbiodinium*. Arrows indicate examples of *Symbiodinium* cells.